Position Matching Estimation for GNSS Positioning in Multipath/Non-Line-Of-Sight Environments

Nabil Kbayer
TeSA/ISAE-SUPAERO
Toulouse, FRANCE
Email: nabil.kbayer@isae.fr

Mohamed Sahmoudi
and Héctor Ortega-González
DEOS/ISAE-SUPAERO
Toulouse, FRANCE

Cédric Rouch
French Space Agency (CNES)
Toulouse, FRANCE

Nabil Kbayer is a PhD student at the French Institute of Aeronautics and Space (ISAE-SUPAERO), University of Toulouse, France. He received his engineer degree in signal processing from ISAE-ENSICA. His research interests include signal processing for positioning in challenging environments, multipath and NLOS mitigation and constructive use for cognitive navigation.

Mohamed Sahmoudi received a PhD in signal processing and communications systems from Paris-Sud Orsay University, France, in collaboration with Telecom Paris in 2004. From 2005 to 2007, he was a post-doctoral researcher fellow on GPS Signal Processing and Navigation at Villanova University, PA, USA. In august 2007, he joined the ETS school of engineering at Montreal, Canada, to lead the research team of precise positioning (RTK and PPP). In 2009, he became an Associate Professor at ISAE-SUPAERO, University of Toulouse, France. Currently his research interests focus on all aspects of signal processing for navigation in harsh environment, weak GNSS signals acquisition and tracking, multi-frequency and multi-GNSS receivers, multipath mitigation and constructive use and multi-sensor fusion for robust navigation.

Héctor Ortega-González is a Telecommunications Engineering student at Telecom BCN (ETSETB), Polytechnic University of Catalonia (UPC), Spain. He is currently carrying out his Final Degree Project at ISAE-SUPAERO. His research interests include signal processing applied to navigation as well as space systems.

Cédric Rouch, graduated in 2013 from the French Civil Aviation University (ENAC) in Toulouse, France. He worked on aircraft flight control law on the behalf of Airbus, and then he joined the CNES Navigation and Telecommunications department in 2015. He is involved in GNSS simulation and positioning performance assessment activities. He is, at present, responsible for the development of the SPRING, a software designed for analysis of systems integrating GNSS positioning. He is also in charge of GNSS measurement campaigns and experiments.

***Abstract*—Recent trends in Global Navigation Satellite System (GNSS) applications in urban environments have led to a proliferation of research works that seek to mitigate the adverse effect of Multipaths (MPs) and non-line-of-sight (NLOS). For such harsh urban settings, this paper proposes an original methodology for constructive use of degraded MP/NLOS signals, instead of their elimination, via a fusion of GNSS pseudoranges (PR) with aided information from a 3D GNSS simulator. First, a 3D GNSS simulator is used to characterize and predict PR measurements over an array of candidate positions in the environment under study. Then, a similarity scoring technique based on least-squares (LS) position matching is applied to score candidate positions. Finally, the final position estimate is retained as the weighted average of the candidate positions with the highest scores. Experiment results using real GNSS data in a deep urban environment confirm the theoretical sub-optimal efficiency of the proposed approach, despite it intensive computational load.**

Keywords: ***GNSS in urban areas; Multipath and NLOS reception; Position Matching; 3D City Models; GNSS simulators***

I. Introduction

The Global Navigation Satellites Systems (GNSS) application for land navigation has grown in popularity in urban areas for their free accessibility and suitable accuracy. Motivated by the significant developments of GNSS-based techniques, satellite positioning is poised to have a wide spectrum of applications in land navigation, intelligent transportation systems (ITS), robots/Drones, Location-Based Services (LBS) and Wireless Sensors Networks (WSN) [1].

User requirements in these environments can be specified from numerous perspectives, including accuracy, integrity, reliability, continuity. These requirements can be very stringent and depends on the specific applications. For instance, GNSS reliability is mandatory especially for applications having impacts on financial, legal or safety-of-life repercussions such as specific car tracking or road user charging (RUC) [2]. Hence, along with the appearance and innovation of new land applications, many of the demands come from urban environments where the processing needs of the received signals are extensively more complex than in open sky environments.

However, the exponential progress of GNSS applications in land navigation is not without major hurdles in its course of development. Indeed, even with this increase in the satellite availability and the improvement of the constellation geometry, GNSS positioning in urban areas suffer from degraded performance because of several problems that persist. Basically, the rapid urbanizing process in many cities hinders existing GNSS-based positioning technologies performances to achieve the technical and regulation requirements for three main reasons, namely satellite masking and signal attenuation, GNSS signal reflections and degraded satellite-user geometry. As GNSS rely on signals received through a Line-Of-Sight (LOS) path, any infringement of this assumption can result in very degraded positioning accuracy. This makes the reception of signal reflections the major hurdle in the development of GNSS in urban areas.

Urban environment, on the whole, consists of narrow streets and high buildings with smooth surfaces that may reflect the transmitted signals. Thus, it is very common that GNSS signals reach the receiver via multiple, direct and/or indirect paths, called Non-Line-Of-Sight (NLOS) in this case. Even though both the NLOS reception and multipath interference

are often grouped together as multipath, they are actually separate phenomena that cause very different ranging errors and different caracteristics [3].

Multipath interference occurs when the transmitted satellite signals are received through multiple replicas which follow different paths than the original satellite-user direct link. These different path are caused by the reflection or diffraction of the direct signals. Such multipaths distort the correlation function between the received composite (direct path plus multipaths) signal and the locally generated reference in the receiver. Theoretically, the magnitudes of multipath error can reach about 0.5 of a code chip depending on the receiver correlation technology [4], [3].

Non-Line-of-Sight (NLOS) is a term to describe a link where there is no visual line-of-sight (LOS) between the transmitting antenna and the receiving antenna. If the line of sight (LOS) is blocked and the satellite signal is received through a reflected NLOS path, the related pseudo-range (PR) measurement will be affected by an additional bias, always positive, potentially unlimited in range and with an magnitude dependent on the propagation environment.

Improvements due to GNSS augmentations and GNSS modernization are reducing many sources of error, leaving multipath and shadowing as significant and sometimes dominant contributors to error. As they usually arise together in urban settings, these two phenomena distort the composite phase of the received signal, introducing errors in pseudorange measurements, and thus producing errors in position, velocity, and time. In view of such technical challenges in urban areas, there is a pressing need for mitigating these unwanted effects to achieve the required positioning accuracy.

In this paper, we propose to use a 3D GNSS Simulator to characterize and estimate these ranging errors. A new position estimation solution will be proposed based on 3D aided information provided from this 3D GNSS Simulator. This proposed method is introduced in the framework of the integration of GNSS observations with information from 3D GNSS simulators.

This paper is divided into five main sections. The first one proposes a review of the state on the MP/NLOS problem. The second section presents the 3D GNSS simulator used in this work. In the third section, we introduce our contribution for positioning in MP/NLOS conditions. The fourth section outlines experimental results obtained in an urban area using the proposed approach and a 3D GNSS simulator. Finally, some conclusions are summarized in section 5.

II. Related Works

A huge amount of researches have been conducted and are still actively ongoing in order to develop methods to overcome these challenges and improve the quality of localization, even in presence of MP/NLOS conditions. Broadly speaking, the literature on the MP/NLOS problem falls in these main categories:

- **MP/NLOS Identification/Detection:** Methods focusing on identifying the contaminated signals and detecting MP and/or NLOS receptions.
- **MP/NLOS Mitigation and Modeling:** Methods focusing on mitigating or modeling MP/NLOS signals.
- **MP/NLOS Weighting:** Methods focusing on down-weighting the unwanted effects of MP/NLOS signals.
- **MP/NLOS Estimation:** Methods focusing on estimating the time-varying MP and NLOS ranging bias.
- **MP/NLOS Constructive Use:** Methods focusing on using constructively these degraded MP/NLOS signals for positioning instead of their elimination, since LOS signals may be too scarce in some situations.

This former type of techniques applied to MP/NLOS problem tends to distinguish between clean Line-of-Sight (LOS) signals and "deteriorated" MP/NLOS signals. These distinction methods can be largely grouped into those using an additional hardware or information sources with the principal positioning system, such as a dual polarization antenna [5], a GNSS antenna array [6] and a sky-pointing camera [7], [8], and those focusing on detecting MP/NLOS signals without using any external information or any additional hardware [9], [10].

The second category considers that it is of utmost importance to characterize and remove MP/NLOS measurement errors. For these reasons, several researches have been conducted and are still ongoing to mitigate the influence of MP/NLOS bias. Most principal works can be largely classified into these three classes: methods using special multipath limiting antennas or hardware [11], [12], [13], [14], receiver-internal correlation techniques in the signal domain [15], [16] and post processing techniques in the measurements domain [17].

The basic idea of MP/NLOS weighting techniques is to assign a low weight to outlier "contaminated" measurements, i.e., a low contribution in the position estimation, while giving a nominal weight or total contribution to "clean measurements" in the PVT computation [18], [19], [20]. Other methodologies have been studied in order to estimate simultaneously the user position and the measurements errors all along the observation interval. MP/NLOS estimation methods may be classified into two categories: methods tending to estimate MP/NLOS in the receiver-internal correlation loops [21] and methods estimating the MP/NLOS errors in the navigation block [22], [23].

Since direct LOS signals may be too scarce in urban environment, a new trend of techniques has recently received some attention in the literature. These methods aim to detect degraded measurements and use them constructively instead of eliminating them [24], [25], [26]. In fact, under poor conditions of satellite visibility, it is more interesting to use constructively these NLOS observables. MP/NLOS Constructive use based techniques totally differ from MP/NLOS mitigation based techniques and MP/NLOS weighting based techniques: using constructively MP/NLOS errors signifies using all available pseudorange measurements without down-weighting any measurements, unlike MP/NLOS weighting

based methods, and without discarding any measurement, contrary to MP/NLOS mitigation based methods.

Among MP/NLOS Constructive Use techniques, new methods exploit the measurements model via aiding information about the geometric environment of reception from 3D city models, as in [24], [27]. However, to deal with the problem of the vicinity of the input point provided to the 3D simulator and the unknown position to be estimated, some studies predict the path delay of the NLOS signals across an array of candidate positions [25], [27], [28], [29], i.e. considering signal reception at multiple candidate positions. The positioning technique is then based on scoring position hypotheses by comparison between observations at the receiver and information provided by the 3D model/3D simulator such as the sky visibility [27], the NLOS signal delay [28], the PR measurements [29].

Another way of exploiting the 3D city model is to predict the NLOS bias via GNSS propagation simulations and then correcting it in the PR measurements [24], [25]. In [24] and [25], we have used the 3D model to predict PR errors and use it constructively on the estimation step. We have used these bias predictions in different ways, including instantaneous corrections, using the mean and variance, and other statistics such as the minimum and maximum bounds as constraints in the estimation process. However, this PR correction step is a sensitive task: poor PR bias predictions may engender an erroneous ranging correction and then may sensitively reduce the position estimation instead of enhancing it [30]. Hence, in this paper, we propose to use a 3D GNSS simulator to consider signal propagation at multiple candidate positions for position hypothesis scoring and final position estimating among these candidate locations.

In this study, we use the 3D GNSS Simulator SPRING [31], provided by the French Space Agency (CNES), to predict these ranging errors in urban areas. These estimated biases are then used to define a position matching estimate. This estimate, called PM-3D, computes a likelihood function over an array of position hypothesis based on the similarity between measured and predicted position information. The proposed estimator gives then an estimation of the final solution over an array of candidates in the position domain. Experimental results show that better performance can be obtained by using the PM-3D even in harsh environment with mixed MP and NLOS receptions.

III. 3D GNSS Simulations

3D city models are 3-dimensional digital representations of terrain surfaces, sites, buildings, vegetation, infrastructure and landscape elements as well as related objects present in cities. Buildings in 3D models are represented by collection of points in 3D space, connected by various geometric entities such as triangles, lines, curved surfaces, etc. It is now possible to integrate into some GNSS propagation simulators detailed highly realistic 3D maps of real environments, such as buildings or infrastructure of cities. This integration will be termed as 3D GNSS simulator.

3D GNSS signal simulators were originally developed to test GNSS receiver algorithms before they were actually implemented. Subsequently, with their complexity, they have been used to better understand the propagation phenomena of GNSS signals and the impact of different sources of noise. Today, thanks to an ever-increasing realism, a new use has emerged: 3D simulators are used as aids to navigation.

3D GNSS deterministic simulators reproduce the interactions with the environment from a physical point of view, by modeling the reflection and diffusion of GNSS signals with the environment [32], [33]. These simulators, based on the propagation laws of electromagnetic signals, reproduce with a high representativity the interactions of GNSS signals with the environment.

In this category, SPRING [31], [34] is a GNSS simulator developed by the French Space Agency (CNES) that has the capability of simulating, via ray-tracing techniques, all paths to be received in a certain input position at a certain time. SPRING is developed jointly with Thales Services, to predict PR errors in urban areas. It allows the simulation of the propagation of the GNSS signals inside a realistic 3D scene for an in depth analysis of the multipath. A reception channel model and a receiver model enable the acquisition and tracking of the signals propagated in the environment in order to calculate pseudoranges, phase and Doppler measurements of the acquired satellites. This simulator is provided by CNES and used in this research work to assist the GNSS receiver in order to enhance positioning performance.

The used 3D in this research work is Toulouse 3D model. This 3D city model is developed by the French National Geographic Institute (IGN). It is based on high resolution images with level 2 of detail (LoD2). Simulated PR measurements are computed thought GNSS signal propagation within the 3D city model and in the wake of signal acquisition and tracking using the receiver model implemented in SPRING. The LOS distance between the satellite and the input position introduced in the software is expressed as the direct path between these two points. As all the other ranging errors (ionospheric, tropospheric, thermal noise...) are not modelled, the PR bias, which is the parameter of main interest in this dissertation, is predicted as the difference between simulated PR measurements and the LOS distance. It must be emphasised that PR receiver bias is omitted in 3D simulation as the receiver is supposed to be synchronized with emitted satellites.

Fig. 1 shows a screen-shot of an example of SPRING simulation in an urban environment. Continuous lines refer to signals received in direct line-of-sight while dotted lines represent signals received through indirect paths. The main steps used for 3D PR bias estimation at each candidate position are summarized in the algorithm 1 below.

IV. PROPOSED POSITIONING ALGORITHM

A. *Effect of MP/NLOS biases on Position estimation*

GNSS is a global technology that allows users over the globe to locate themselves to navigate and have a mean for synchronization on a common time reference. A user

Algorithm 1 3D GNSS Simulation

Inputs: GPS Time, Satellite ephemeris, 3D city Model and input position $\mathbf{x}_i$

Output: 3D bias $\mathbf{b}_{3D}(\mathbf{x}_i)$

1: **Compute satellite positions**

2: **Determine LOS distance between each satellite and the input position**
For each satellite Sat_i, compute $PR_i^{LOS} = \|\mathbf{x}_i - \mathbf{x}_i^{Sat_i}\|_2$

3: **Predict 3D received PR measurements**
For each satellite Sat_i, predict PR_i^{3D}, using the 3D model, ray-tracing algorithm and the receiver model implemented in SPRING

4: **Compute PR bias**
As all the other ranging errors are not modelled, PR bias is the difference between predicted PR measurements and LOS distance: $[\mathbf{b}_{3D}(\mathbf{x}_i)]_i = PR_i^{3D} - PR_i^{LOS}$

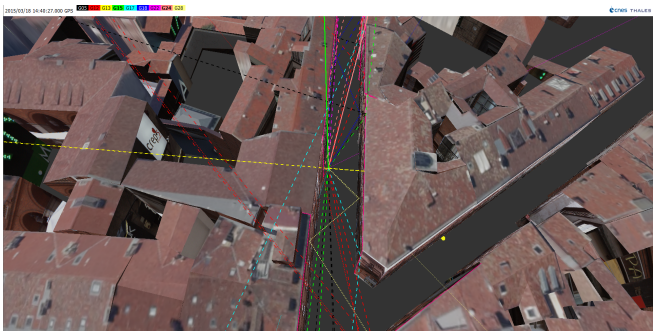

Fig. 1: 3D GNSS Simulation using SPRING by considering both diffractions and multiple reflections

equipped with proper equipment is able to access emitted satellite positioning information, decode them and solve the problem of position determination. GNSS position determination resides on the trilateration concept using at least four LOS measurements from known satellites locations. However, signal degradation is more prominent in harsh environments, as opposed to open sky environments, inducing then an additional MP/NLOS ranging bias. Considering N emitting GNSS satellites, the following linearized equation formulates the satellite positioning problem at each time step [35]:

$$\mathbf{y} = \mathbf{H}\mathbf{x} + \mathbf{v} + \mathbf{b} \tag{1}$$

Where, throughout this paper, the $[M, 1]$ state vector $\mathbf{x} = (x - x_0, y - y_0, z - z_0, b_{Rx})^T$ contains the parameters of primary interest, i.e. the three coordinates of the user position $(x, y, z)^T$ and the receiver clock bias b_{Rx}, which is common between all the received satellites. $\mathbf{y} = (y_1, \cdots, y_N)^T$ is the $[N, 1]$ linearised pseudorange (PR) measurements vector. $\mathbf{H}$ contains the unit line-of-sight (LOS) vectors between the satellites and the previous user position $\mathbf{x_0} = (x_0, y_0, z_0)^T$. This matrix describes the linear connection between the measurements $\mathbf{y}$ and the unknowns $\mathbf{x}$. $\mathbf{b} = (b_1, \cdots, b_N)^T$refers to the additional measurement bias caused by MP/NLOS receptions $[N, 1]$ and is commonly called PR bias. $\mathbf{v} = (v_1, \cdots, v_N)^T$ is the measurement noise, supposed to be a white Gaussian noise characterized by a known covariance matrix $\mathbf{R} = E\{\mathbf{v}\mathbf{v}^T\}$.

The likelihood cost function for user position estimation is straightforward:

$$\begin{aligned} J(\mathbf{y}|\mathbf{x}, \mathbf{b}) &= \|\mathbf{y} - \mathbf{H}\mathbf{x} - \mathbf{b}\|^2_{\mathbf{R}^{-1}} \\ &= (\mathbf{y} - \mathbf{H}\mathbf{x} - \mathbf{b})^T \mathbf{R}^{-1} (\mathbf{y} - \mathbf{H}\mathbf{x} - \mathbf{b}) \end{aligned} \tag{2}$$

The maximum likelihood estimate (ML) is the estimate that minimizes the above likelihood cost function as:

$$\hat{\mathbf{x}}_{ML} = \underset{\mathbf{x}}{\operatorname{argmin}}\, J(\mathbf{y}|\mathbf{x}, \mathbf{b}) = \mathbf{H}^+(\mathbf{y} - \mathbf{b}) \tag{3}$$

where $\mathbf{H}^+ = (\mathbf{H}^T\mathbf{R}^{-1}\mathbf{H})^{-1}\mathbf{H}^T\mathbf{R}^{-1}$ is the pseudo-inverse of $\mathbf{H}$ weighted by the inverse of the measurements covariance matrix $\mathbf{R}$. The mean square error (MSE) of this estimator can be expressed as:

$$\begin{aligned} MSE[\hat{\mathbf{x}}_{ML}] &= E\{(\hat{\mathbf{x}}_{ML} - \mathbf{x})(\hat{\mathbf{x}}_{ML} - \mathbf{x})^T\} \\ &= (\mathbf{H}^T\mathbf{R}^{-1}\mathbf{H})^{-1} \end{aligned} \tag{4}$$

The ML estimate can be seen also as a least squares solution applied on corrected ranging measurements: a sum of a bias free-estimate termed as the Least Squares (LS) estimate $\hat{\mathbf{x}}_{LS} = \mathbf{H}^+\mathbf{y}$, i.e. computed as if no additional bias were present, and a bias-correction term $\mathbf{H}^+\mathbf{b}$.

In general, the bias-correction term cannot be computed since the MP/ NLOS is unknown, highly variable and hard to be estimated. Thus, the ML computation is impossible and only a bias free-estimate can be performed. This bias free-estimate is equal to the least squares estimator (LS) of problem (1). This estimator is less efficient than the optimal ML estimate. Indeed, we have the following inequality satisfied by the overall mean square error OMSE (trace of the MSE matrix):

$$\begin{aligned} OMSE[\hat{\mathbf{x}}_{LS}] &= \mathrm{Tr}\{(\mathbf{H}^T\mathbf{R}^{-1}\mathbf{H})^{-1}\} + \mathrm{Tr}\{\mathbf{H}^+ E\{\mathbf{b}\mathbf{b}^T\}(\mathbf{H}^+)^T\} \\ &\geq \mathrm{Tr}\{(\mathbf{H}^T\mathbf{R}^{-1}\mathbf{H})^{-1}\} = OMSE[\hat{\mathbf{x}}_{ML}] \end{aligned} \tag{5}$$

This previous equation illustrates the effect of MP/NLOS biases on the final positioning error. Indeed, without knowing these biases, we have the previous inequality and therefore the LS estimation, under MP/NLOS conditions, will be degraded. In view of such technical challenges, there is a pressing need to counteract the disadvantages of these GNSS degradations, namely MP/NLOS reception, and achieve user requirements in harsh environments: This is one of the principal motivation of the use of 3D simulators as indicators on signal reception statuts in this research work.

B. Position Matching estimate (PM-3D)

Since the computation of the likelihood cost function (2) is theoretically impossible without any prior information on the PR bias, we propose a new cost function that approximates the theoretical maximum-likelihood cost function. To do that, we make use of the 3D GNSS simulator SPRING. This proposed method makes use of an array of candidate position to define the final estimate among this grid, based on a defined matching metric. The matching metric is the objective of this work. In this work, we define a matching metric based on position

similarity that will be detailed in this section. The proposed Position Matching estimate (PM-3D) follows these steps:

- **Step 1: Outdoor Candidate Positions Definition**
  We define a 2D array of equidistant outdoor candidate positions $\Gamma = \{\mathbf{x}_i = (x_i, y_i, z)^T\}$ in the environment under study, using the software Q-GIS and the 3D city model.
- **Step 2: 3D PR Bias Prediction**
  For each candidate position, we predict the corresponding PR bias using SPRING to obtain a bank of 3D PR bias: $\Omega = \{\mathbf{b}_{3D}(\mathbf{x}_i) = (\mathbf{b}_{3D}(\mathbf{x}_i)_1, \cdots, \mathbf{b}_{3D}(\mathbf{x}_i)_N)^T\}$.
- **Step 3: Define a Reference Satellite**
  Based on C/N0 ratios or elevation angles, we define a reference satellite which is the satellite having the most reliable and "healthy" PR measurements.
- **Step 4: Estimate 3D bias prediction uncertainty**
  It is evident that the predicted bias and errors from the 3D propagation model cannot be instantaneous and accurate. The quality and reliability of the PR bias estimation depends on many factors such as the accuracy of signal propagation modeling, the precision of 3D city modeling, receiver setting, etc... Since the proposed approach depends on the accuracy of the simulation, we propose to estimate the uncertainty on bias estimation provided by the 3D GNSS simulator. Preliminary tests on the evaluation of the performance of this tool show that PR biases of high elevation signals are usually correctly estimated, as the signal have less interactions with the environment surrounding the receiver contrary to low or medium elevation signals. Then, we propose the following formula as estimation for this uncertainty on bias prediction. $\alpha_{Max-Inaccuracy}$ refers to the highest error on bias estimation.

$$\tilde{\delta}_{3D} = \alpha_{Max-Inaccuracy} \exp(\mathbf{Elev}/(\mathbf{Elev} - 90)) \quad (6)$$

  where $\mathbf{Elev}$ refers to satellite elevation angle in degrees. Similarly, we can also estimate this uncertainty on bias prediction based on the C/N0 ratio as:

$$\tilde{\delta}_{3D} = \alpha_{Max-Inaccuracy} 10^{\frac{C/N0}{C/N0_{Max}}} \quad (7)$$

- **Step 5: Position Matching Cost Function**
  Based on predicted 3D PR bias, we define the following cost function as:

$$\begin{aligned} &\Psi : \Gamma \rightarrow \mathbb{R} \\ &\mathbf{x}_i \mapsto \Psi(\mathbf{y}|\mathbf{x}_i, \mathbf{b}_{3D}(\mathbf{x}_i)) = \|\mathbf{H}^+(\mathbf{y} - \mathbf{b}_{3D}(\mathbf{x}_i)) - \mathbf{x}_i\|_2^2 \\ &\qquad = \|\mathbf{H}^+(\mathbf{H}\mathbf{x}_i + \mathbf{b}_{3D}(\mathbf{x}_i)) - \hat{\mathbf{x}}_{LS}\|_2^2 \end{aligned} \quad (8)$$

  Where $\hat{\mathbf{x}}_{LS} = \mathbf{H}^+\mathbf{y} = (\mathbf{H}^T\mathbf{R}^{-1}\mathbf{H})^{-1}\mathbf{H}^T\mathbf{R}^{-1}\mathbf{y}$ is the LS solution of the GNSS problem. This new cost function is based on predicted 3D PR bias. This metric represents a projection of the similarity between the 3D predicted PR measurement $\mathbf{H}\mathbf{x}_i + \mathbf{b}_{3D}(\mathbf{x}_i)$ from the 3D GNSS simulation and the received PR measurements $\mathbf{y}$. The physical interpretation of this metric will be also provided in the next sub-section.
  To reduce the estimation complexity, a classical hypothesis consists of using the 3D GNSS simulator to avoid the estimation of the height information. Given the horizontal coordinates of each grid point, a height is associated to this point using the 3D city model which avoids the computational load over a 3D search area. Then, the receiver clock bias is eliminated by proceeding to a differentiation of all ranging measurements across satellites using a reference satellite. This allows to reduce the computation of the cost function Ψ in (8) and gives a new modified position matching cost function:

$$\begin{aligned} \tilde{\Psi}(\mathbf{y}|\mathbf{x}_i, \mathbf{b}_{3D}(\mathbf{x}_i)) = \|(\mathbf{H}^+ - \mathbf{H}^+(ref,:))(\mathbf{y} - y_{ref} \\ - \mathbf{b}_{3D}(\mathbf{x}_i) - \tilde{\delta}_{3D}) - \mathbf{x}_i\|_2^2 \end{aligned} \quad (9)$$

  Where y_{ref} is the ranging measurement of the reference satellite and $\mathbf{H}^+(ref,:)$ is the row of matrix $\mathbf{H}^+$, corresponding to the reference satellite.
- **Step 6: Final Estimate**
  Considering the final position as the candidate position having the lowest score, i.e. minimizing the approximate maximum-likelihood cost function in (9), is risky. Therefore, we propose to estimate the final PM-3D solution as a weighted average of the candidate positions with the lowest scores, i.e. the highest PR measurements matching. In fact, by evaluating the previous cost function on the array of candidate positions, we define the position matching (PM) estimator as:

$$\hat{\mathbf{x}}_{PM} = \frac{\sum_{i=1}^{N_{Th}} (\tilde{\Psi}(\mathbf{y}|\mathbf{x}_i^\Omega) < Th)\mathbf{x}_i^\Omega}{\sum_{i=1}^{N_{Th}} (\tilde{\Psi}(\mathbf{y}|\mathbf{x}_i^\Omega) < Th)} \quad (10)$$

  Where Th is the threshold used for selecting the lowest scores, N_{Th} corresponds to the number of grid points with a matching score lower than the threshold Th and the set $\Omega = \{\mathbf{x}_i^\Omega, i = 1, \cdots, N_{Th}\}$ refers to the subset of candidate positions with the lowest scores. This PM estimator represents a weighted average of the candidate positions with the lowest scores, i.e. the highest matching.

C. Theoretical performance: Convergence to ML estimator

Since the bias estimation by 3D simulations cannot be accurate, we define the uncertainty on the bias estimation as:

$$\delta_{3D} = \|\mathbf{b} - \mathbf{b}_{3D}(\mathbf{x})\|_{\mathbf{R}^{-1}}^2 \quad (11)$$

With this in mind, it is interesting to investigate the theoretical performance of this proposed algorithm compared to the ML estimator. We can show the following lemma:

$$\mathrm{Tr}\{MSE(\hat{\mathbf{x}}_{PM})\} \underset{\delta_{3D} \rightarrow 0}{\longrightarrow} \mathrm{Tr}\{MSE(\hat{\mathbf{x}}_{ML})\} \quad (12)$$

Proof: See Appendix A.

The previous relation (12) demonstrates that, conditioned by 3D GNSS simulator accuracy, the overall mean square error (trace of the MSE matrix) of the PM estimator converges to the minimum overall mean square error of the ML solution of problem (1).

D. Physical Interpretation

The position matching metric in (9) evaluates the similarity between each point of the set of candidate positions $\Gamma = \{\mathbf{x}_i = (x_i, y_i, z)^T\}_i$ and each point of the set of calculated positions $\Gamma_1 = \{\mathbf{H}^+(\mathbf{y} - \mathbf{b}_{3D}(\mathbf{x}_i))\}_i$ obtained via LS-type projection (using the projection operator $\mathbf{H}^+$) applied to corrected PR measurements using 3D predicted MP/NLOS biases from SPRING simulation. It also evaluates the similarity between the conventional LS solution and the set of solutions obtained by applying an "LS" type projection to simulated PR measurements by SPRING-3D simulation $\{(\mathbf{H}\mathbf{x}_i + \mathbf{b}_{3D}(\mathbf{x}_i))\}_i$. PM-3D positioning technique is then based on position matching between the LS solution and a simulated LS solutions, or similarly between candidate position and position obtained by PR measurement correction, over an array of candidate positions.

If the GNSS simulator is sufficiently accurate, the projection of the "LS" type applied to simulated PR measurements (predicted by the SPRING-3D simulator) obtained by SPRING simulation at a candidate position $\mathbf{x}_i$ close to the true position $\mathbf{x}$, will give a solution close to the LS solution obtained by applying the LS algorithm to true PR measurements received at the true unknown position. The physical interpretation of PM-3D algorithm is explained in 2(a). As a way of illustration, a block diagram of our proposed PM-3D algorithm is given in Fig. 2(b).

Finally, the proposed approach is summarized in the algorithm 2 below:

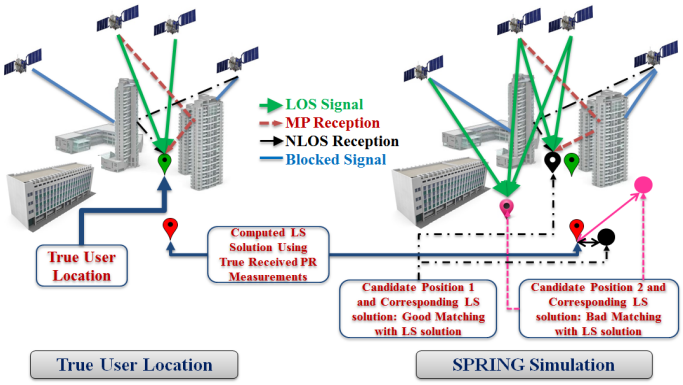

(a) PM-3D: Physical interpretation

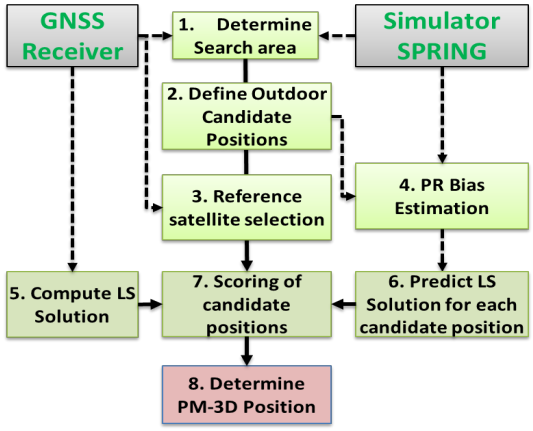

(b) PM-3D algorithm block diagram

Fig. 2: Position Matching algorithm

Algorithm 2 PM Estimation

Inputs: $\mathbf{y}, \mathbf{H}$ and $\tilde{\delta}_{3D}$
Output: $\hat{\mathbf{x}}_{PM}$

1: **Define search area and grid of candidate positions**
Define an array of 2D points $\Gamma = \{\mathbf{x}_i = (x_i, y_i, z)^T\}$
2: **Estimate a bank of PR biases over candidate positions**
Estimate PR biases, using 3D GNSS simulations, for the considered array of candidate positions
$\Omega = \{\mathbf{b}_{3D}(\mathbf{x}_i) = (\mathbf{b}_{3D}(\mathbf{x}_i)_1, \cdots, \mathbf{b}_{3D}(\mathbf{x}_i)_N)^T\}$
3: **Reference satellite selection using elevation criterion**
4: **Likelihood scoring for each candidate position**
Compute $\tilde{\Psi}(\mathbf{y}|\mathbf{x}_i)$ using (9)
5: **PM-3D position estimation**
Estimate PM-3D solution $\hat{\mathbf{x}}_{PM}$ using (10)

E. Comparison Algorithm

Considered among the most mature 3D model based positioning approaches, Shadow Matching solution [36] uses 3D building models to improve cross-track positioning accuracy in harsh environments by predicting which satellites are visible from different candidate locations and comparing this information with the measured satellite visibility to determine the final user solution. This positioning approach is based on a GNSS and 3D model fusion for satellite shadows scoring of candidate positions. Shadow Matching is based on comparison between observed satellite visibility based on GNSS signal-to-noise measurements and signal availability predictions, at different candidate locations, derived from a 3D city model [37]. By achieving accurate cross-street positioning in urban canyons, it was implemented for smartphone applications [38], [39]. The basic Shadow-Matching approach can summarized in the algorithm 3 below.

In this experimentation, we have used our implementation of Shadow Matching solution to compare and assess the performance of our proposed algorithm. The Shadow Matching algorithm has been implemented using GPS and GLONASS signals. Our proposed PM-3D has been implemented using GPS signals only since 3D GNSS simulation using GLONASS constellation is not yet optimized in the current version of the simulator.

Algorithm 3 Shadow-Matching (SM) Estimation

Inputs: $\mathbf{y}, \mathbf{H}$, C/N0 Coefficients (for satellite visibility)
Output: $\hat{\mathbf{x}}_{SM}$

1: **Define search area and grid of candidate positions**
2: **Building Boundaries (BB) computation**
For each candidate position, predict building edges using the 3D city model for one area of the map (computed only once)
3: **Predict satellite visibility**
For each candidate position, predict satellite visibility using the Building Boundaries information
4: **Measure satellite visibility**
Use C/N0 ratios to determine the observed satellite visibility
5: **Scoring of candidate positions**
Based on matching between predicted and measured satellite visibility, score each candidate point
6: **Final position estimation**
Estimate the final user position based on weighting the positions with having the highest scores

V. EXPERIMENTAL RESULTS

A. General Experimental Setup

To evaluate the proposed solution, a dynamic positioning test was conducted in an urban environment. GPS L1 C/A code PR measurements were collected on March 18, 2015 around Capitole Square in Toulouse. The GNSS receivers used are the following:

- **A UBLOX 6T Receiver:** a low cost receiver recording only GPS constellation. L1 C/A code PR measurements were recorded at a rate of 4 Hz.
- **A Novatel SPAN system:** include a a Novatel single-constellation DGPS receiver tightly integrated with an IMU-FSAS inertial unit (from iMAR). The data are sampled at a rate of 10 Hz. Differential correction were performed using a reference static antenna. We consider the trajectory provided by the Novatel system as the reference trajectory for comparison with our algorithm.

All data processing was accomplished using Matlab. For this validation test, we have selected a trajectory along an urban environment characterized by narrow streets and medium-height buildings, which are predominantly the down-towns of European cities. We have used the elevation angle as criterion for reference satellite selection. The chosen area represents a harsh environment with narrow streets and medium-height buildings alongside the streets. An overview of the considered urban area and the temporal number of usable GPS satellites during this test in the deep urban section are shown in Fig. 3.

For illustration of the used grid of candidate positions, Fig. 4 shows the used array of positions. In this experimental evaluation of our algorithm, we have used 1600 candidate positions in a square area in the region of interest. These positions are uniformly distributed in this search area with a spacing of 1m. A pre-processing algorithm is implemented to exclude the

(a) Tested Urban Environment (White line: Reference trajectory)

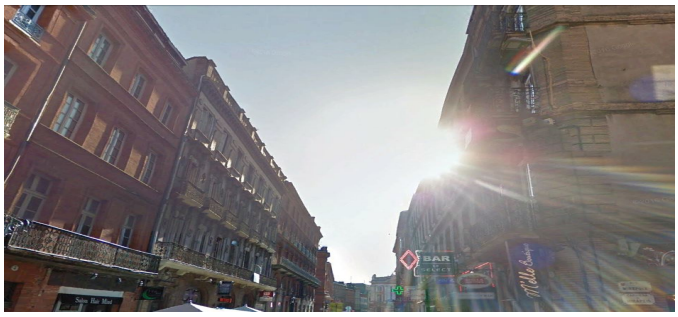

(b) Sky-view of the urban section

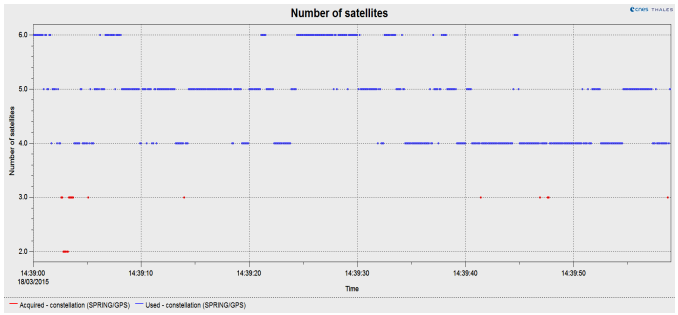

(c) Temporal number of GPS satellites

Fig. 3: Overview of experimental setup

indoor points based on the 3D model of the city. Hence, this grid of candidate positions contains only outdoor locations. The red dots refer to the used reference trajectory, while the white dots represent the considered candidate positions.

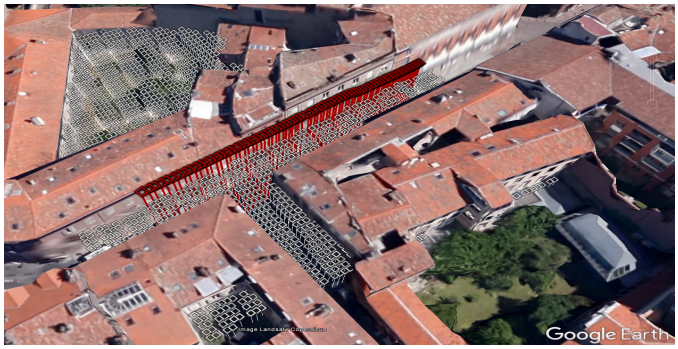

Fig. 4: Used Array of candidate positions

B. Performances of the Proposed Solution

For this validation test, we have compared the positioning performance using PM-3D solution without 3D simulation error correction, i.e. $\delta_{3D} = 0$, Shadow-Matching solution (SM-3D) and a conventional Least-Squares solution. Fig. (5) shows the cumulative distribution function of the horizontal position errors of the proposed PM-3D solution, Shadow-Matching solution (SM-3D) and the conventional solution in the considered scenario.

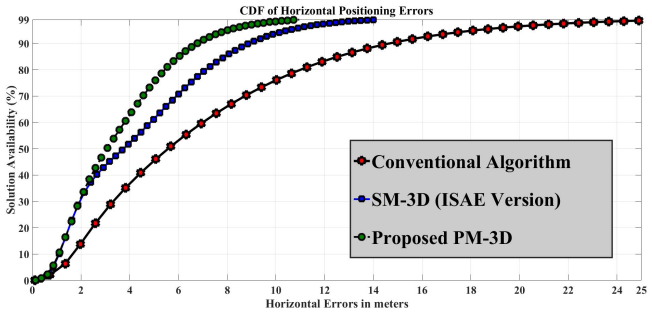

Fig. 5: CDF of Horizontal Positioning Errors

It is apparent from the CDF figure in Fig. (5) that our approach PM-3D gives more positioning performance compared to the conventional GNSS solution. PM-3D positioning performance in this scenario is comparable to that of the Shadow-Matching solution (SM-3D: ISAE Version). We compare horizontal positioning errors (HPE) for these estimators in this scenario with position accuracy obtained using industrial solutions of the UBLOX and Septentrio receivers. Results are shown in Table I. We notice that PM-3D outperforms, in average, all solutions even the industrial solutions.

TABLE I: HORIZONTAL POSITIONING PERFORMANCES

	PM-3D	**SM-3D**	**UBLOX**	**Conventional Algorithm**
Mean of HPE [m]	3.41	4.22	7.27	6.6
HPE at 95% [m]	6.36	7.95	11.65	14.66
HPE at 97% [m]	6.5	9.15	11.85	15.78
HPE at 99% [m]	8.64	9.56	12.41	18.32

The scoring map of the proposed PM-3D solution and the different solutions for a fixed time epoch is shown in Fig. (6).

The previous example illustrates the effectiveness of the proposed PM-3D algorithm even in degraded MP/NLOS conditions. Positioning performance of the PM-3D estimator exceeds that of receiver solution (very good and reliable positioning solutions in general). Better accuracy enhancement using PM-3D algorithm can be obtained by applying a 3D bias uncertainty prediction $\tilde{\delta}_{3D}$ using either the model (6) or the model (7). Taken into account that the 3D simulator SPRING is continuously improved by CNES, this performance obtained by PM-3D might eventually reach more optimal positioning accuracy.

Despite this performance enhancement, this proposed PM-3D algorithm is computationally intensive, especially with

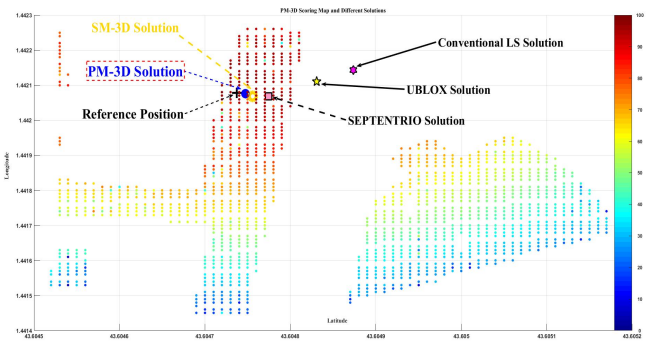

Fig. 6: PM-3D scoring map with different estimation solution for a fixed time epoch

high grid resolution and size, because of bias estimations using 3D simulations. In a natural way, positioning accuracy depends highly on the defined grid of positions. As way of comparison, Table II gives the computational loads of PM-3D compared to SM-3D for the same grid of positions. Nevertheless, this method can be easily implemented on a server mode and send the 3D biases to the mobile receiver to compute its position.

TABLE II: Computational loads of PM-3D and SM-3D

	PM-3D (SPRING Simulation)	**SM-3D (Building Boundary)**
Software	SPRING V4.1.0.7137	Matlab 2013a
CPU	Core(TM) i7-4770 3.4GHz	Core(TM) i5-3470 3.2GHz
Time [s]	10640 ($2h57min$)	3981.65 ($1h6min$)

VI. Conclusion

Stand-Alone GNSS positioning algorithms give a good compromise between positioning accuracy and processing (implementation) simplicity but are unfortunately ineffective in urban environments with reduced visibility of satellites and excessive MP/NLOS errors. In these cases, the use of an external source of information is mandatory for the continuity of navigation. The state of the art is rich by GNSS hybridization methods with inertial sensors, cameras, scan lasers or other sensors. Given the limit of low-cost inertial sensors and the complexity of a tight GNSS/INS hybridization, we propose in this study as an alternative the exploitation of the characteristics of the receiver environment using the 3D GNSS simulator SPRING.

In this regard, this research proposes a 3D GNSS simulator/GNSS hybridization scheme based on scoring of an array of candidate positions using the 3D information from the 3D GNSS simulator. The basic idea is to introduce a grid of input positions to the SPRING-3D GNSS simulator to predict the MP/NLOS biases and retain the candidate position with the best similarity based on a matching score. This last is proposed to be a position matching scoring between the conventional LS solution, obtained from received PR measurements, and a set of LS positions based on 3D simulated pseudoranges provided by SPRING-3D. The key strength of this approach is its sub-optimal effectiveness, which was been proven theoretically and using real GNSS data. Notwithstanding the significant

computational loads, this approach can be implemented in server mode for 3D GNSS simulation.

In terms of directions for future research, further works could focus on enhancing the propagation simulation to reach a higher positioning performance using our approach.

ACKNOWLEDGEMENTS

The authors would like to thank the French Space Agency (CNES) for funding this research project: SPRING Usage for Modeling Multipath Effects on a Receiver (SUMMER). We would like also to thank UCL Engineering's Space Geodesy and Navigation Laboratory (SGNL) for their kind support with problems related to 3D modeling.

APPENDIX A

We start by computing the expression of $\hat{\mathbf{x}}_{PM}$:

$$\hat{\mathbf{x}}_{PM} = \underset{\mathbf{x}_i}{\operatorname{argmin}}\{\frac{\partial}{\partial \mathbf{x}_i}(\Psi(\mathbf{y}|\mathbf{x}_i, \mathbf{b}_{3D}(\mathbf{x}_i)) = 0)\}$$

We compute the derivative of the cost function:

$$\frac{\partial}{\partial \mathbf{x}_i}(\Psi(\mathbf{y}|\mathbf{x}_i, \mathbf{b}_{3D}(\mathbf{x}_i))) = -2\mathbf{H}^{+}(\mathbf{H} + \frac{\partial}{\partial \mathbf{x}_i}\mathbf{b}_{3D}(\mathbf{x}_i))\mathbf{R}^{-1}\mathbf{K}(\mathbf{x}_i)$$

Where $\mathbf{K}(\mathbf{x}_i) = \mathbf{H}^{+}(\mathbf{y} - \mathbf{b}_{3D}(\mathbf{x}_i)) - \mathbf{x}_i$. Then, we get the following expression for the position matching estimate:

$$\mathbf{K}(\hat{\mathbf{x}}_{PM}) = 0 \iff \hat{\mathbf{x}}_{PM} = \mathbf{H}^{+}(\mathbf{y} - \mathbf{b}_{3D}(\hat{\mathbf{x}}_{PM}))$$

Since the MSE matrix is diagonal, the overall mean square error of the PM estimation is expressed as:

$$\begin{aligned}\operatorname{Tr}\{MSE[\hat{\mathbf{x}}_{PM}]\} &= \operatorname{Tr}\{E[(\hat{\mathbf{x}}_{PM} - \mathbf{x})(\hat{\mathbf{x}}_{PM} - \mathbf{x})^T]\} \\ &= E[\|\hat{\mathbf{x}}_{PM} - \mathbf{x}\|_2^2]\end{aligned}$$

The PM estimation error can be expressed as:

$$\begin{aligned}\|\hat{\mathbf{x}}_{PM} - \mathbf{x}\|_2^2 &= \|\hat{\mathbf{x}}_{PM} - \mathbf{H}^{+}\mathbf{H}\mathbf{x}\|_2^2 \\ &= \|\mathbf{H}^{+}(\mathbf{b} - \mathbf{b}_{3D}(\hat{\mathbf{x}}_{PM}) + \mathbf{n})\|_2^2\end{aligned}$$

The previous expression gives:

$$\operatorname{Tr}\{MSE[\hat{\mathbf{x}}_{PM}]\} \leq E\{\|\mathbf{H}^{+}(\mathbf{b} - \mathbf{b}_{3D}(\hat{\mathbf{x}}_{PM}))\|_2^2\} + E\{\|\mathbf{H}^{+}\mathbf{n}\|_2^2\}$$

By developing the two parts of this inequality, we show that:

$$\begin{cases} E\{\|\mathbf{H}^{+}\mathbf{n}\|_2^2\} & = \operatorname{Tr}\{(\mathbf{H}^T\mathbf{R}^{-1}\mathbf{H})^{-1}\} \\ & = \operatorname{Tr}\{MSE[\hat{\mathbf{x}}_{ML}]\} \\ E\{\|\mathbf{H}^{+}(\mathbf{b} - \mathbf{b}_{3D}(\hat{\mathbf{x}}_{PM}))\|_2^2\} & = \operatorname{Tr}\{(\mathbf{H}^{+}E[\delta_{3D}^{PM}(\delta_{3D}^{PM})^T](\mathbf{H}^{+})^T)\} \end{cases}$$

Where $\delta_{3D}^{PM} = \mathbf{b} - \mathbf{b}_{3D}(\hat{\mathbf{x}}_{PM})$. Besides, we have the following inequality for all candidate positions:

$$\|\mathbf{b}-\mathbf{b}_{3D}(\mathbf{x}_i)\|_{\mathbf{R}^{-1}}^2 \leq \|\mathbf{b}-\mathbf{b}_{3D}(\mathbf{x})\|_{\mathbf{R}^{-1}}^2 + \|\mathbf{b}_{3D}(\mathbf{x}_i)-\mathbf{b}_{3D}(\mathbf{x})\|_{\mathbf{R}^{-1}}^2$$

And then, we deduce that:

$$\begin{aligned}\|\delta_{3D}^{PM}\|_{\mathbf{R}^{-1}}^2 &= \min_{\mathbf{x}_i} \|\mathbf{b} - \mathbf{b}_{3D}(\mathbf{x}_i)\|_{\mathbf{R}^{-1}}^2 \\ &\leq \delta_{3D} + \min_{\mathbf{x}_i} \|\mathbf{b}_{3D}(\mathbf{x}_i) - \mathbf{b}_{3D}(\mathbf{x})\|_{\mathbf{R}^{-1}}^2 \leq (1+\eta)\delta_{3D}\end{aligned}$$

where $\eta \ll 1$ and then relation (12) is proven.

REFERENCES

[1] GSA, "GNSS Market Report Issue 5," GSA, Tech. Rep., May, 2017.
[2] Toll Collect, Germany, "Service on the road," https://www.toll-collect.de/en, accessed: 2017-06-01.
[3] P. Groves, "Multipath vs. NLOS signals. How Does Non-Line-of-Sight Reception Differ from Multipath Interference," *Inside GNSS Magazine*, pp. 40–42, November/December 2013.
[4] B. W. Parkinson and J. J. Spilker, *Global Positioning System: Theory and Applications*. Progress in Astronautics and Aeronautics, 1996.
[5] Z. Jiang and P. D. Groves, "NLOS GPS signal detection using a dual-polarisation antenna," *GPS Solutions*, vol. 18, no. 1, pp. 15–26, 2014.
[6] M. H. Keshvadi, A. Broumandan, and G. Lachapelle, "Analysis of GNSS beamforming and Angle of Arrival Estimation in Multipath Environements," in *Proceedings of ION ITM 2011*.
[7] J. Marais, M. Berbineau, and M. Heddebaut, "Land mobile gnss availability and multipath evaluation tool," *IEEE Transactions on Vehicular Technology*, vol. 54, no. 5, pp. 1697–1704, Sept 2005.
[8] J. I. Meguro, T. Murata, J. I. Takiguchi, Y. Amano, and T. Hashizume, "GPS Multipath Mitigation for Urban Area Using Omnidirectional Infrared Camera," *IEEE Transactions on Intelligent Transportation Systems*, vol. 10, no. 1, pp. 22–30, March 2009.
[9] P. D. Groves, Z. Jiang, L. Wang, and M. K. Ziebart, "Intelligent Urban Positioning using Multi-Constellation GNSS with 3D Mapping and NLOS Signal Detection," in *Proceedings of the 25th International Technical Meeting of The Satellite Division of the Institute of Navigation (ION GNSS 2012)*, no. 458 - 472.
[10] P. D. Groves and Z. Jiang, "Height Aiding, C/N0 Weighting and Consistency Checking for GNSS NLOS and Multipath Mitigation in Urban Areas," *Journal of Navigation*, pp. 653–659, 2013.
[11] J. Moreau, S. Ambellouis, and Y. Ruichek, "Fisheye-Based Method for GPS Localization Improvement in Unknown Semi-Obstructed Areas," *Sensors*, 2017.
[12] S. Peyraud, D. Bétaille, S. Renault, M. Ortiz, F. Mougel, D. Meizel, and F. Peyret, "About non-line-of-sight satellite detection and exclusion in a 3D map-aided localization algorithm," *Sensors*, vol. 13, no. 1, pp. 829–847, 2013.
[13] A. Konovaltsev, F. Antreich, and A. Hornbostel, "Performance Assessment of Antenna Array Algorithms for Multipath and Interference Mitigation," in *2nd Workshop on GNSS Signals & Signal Processing - GNSS SIGNALS'2007*, 2007.
[14] M. Sahmoudi and M. G. Amin, "Optimal Robust Beamforming for Interference and Multipath Mitigation in GNSS Arrays," in *2007 IEEE International Conference on Acoustics, Speech and Signal Processing - ICASSP '07*, vol. 3, April 2007, pp. III–693–III–696.
[15] M. S. Braasch, "Performance comparison of multipath mitigating receiver architectures," in *2001 IEEE Aerospace Conference Proceedings (Cat. No.01TH8542)*, vol. 3, 2001, pp. 3/1309–3/1315 vol.3.
[16] M. Bhuiyan, *Analysis of Multipath Mitigation Techniques for Satellite-based Positioning Applications*, ser. Tampere University of Technology. Publication. Tampere University of Technology, 9 2011.
[17] I. Guvenc and C. C. Chong, "A Survey on TOA Based Wireless Localization and NLOS Mitigation Techniques," *IEEE Communications Surveys Tutorials*, vol. 11, no. 3, pp. 107–124, rd 2009.
[18] Y. Gao, "A new algorithm of Receiver Autonomous Integrity Monitoring(RAIM) for GPS navigation," *ION GPS-91*, 1991.
[19] G.-L. Sun and W. Guo, "Bootstrapping M-estimators for reducing errors due to non-line-of-sight (NLOS) propagation," *IEEE Communications Letters*, vol. 8, no. 8, pp. 509–510, 2004.
[20] T. Perala, *Robust Kalman-type filtering in positioning applications*. INTECH Open Access Publisher, 2010.
[21] R. D. Van Nee, J. Siereveld, P. C. Fenton, and B. R. Townsend, "The multipath estimating delay lock loop: approaching theoretical accuracy limits," in *Position Location and Navigation Symposium, 1994., IEEE*, 1994, pp. 246–251.
[22] A. Giremus and J. Y. Tourneret, "Joint detection/estimation of multipath effects for the Global Positioning System," in *Proceedings. (ICASSP '05). IEEE International Conference on Acoustics, Speech, and Signal Processing, 2005.*, vol. 4, March 2005, pp. iv/17–iv/20 Vol. 4.
[23] A. Giremus, J.-Y. Tourneret, and V. Calmettes, "A particle filtering approach for joint detection/estimation of multipath effects on gps measurements," *IEEE Transactions on Signal Processing*, vol. 55, no. 4, pp. 1275–1285, 2007.

[24] A. Bourdeau, M. Sahmoudi, and J.-Y. Tourneret, "Constructive use of GNSS NLOS-multipath: Augmenting the navigation Kalman filter with a 3D model of the environment," in *15th International Conference on Information Fusion (FUSION), 2012*. IEEE, 2012, pp. 2271–2276.

[25] N. Kbayer, M. Sahmoudi, and E. Chaumette, "Robust GNSS Navigation in Urban Environments by Bounding NLOS Bias of GNSS Pseudoranges Using a 3D City Model ," in *Proceeding of ION GNSS 2015*, September 2015.

[26] Y. Ng and G. X. Gao, "Direct Position Estimation Utilizing Non-Line-of-Sight (NLOS) GPS Signals," in *Proceedings of the 29th International Technical Meeting of The Satellite Division of the Institute of Navigation (ION GNSS+ 2016)*.

[27] M. Adjrad and P. D. Groves, "Intelligent Urban Positioning using Shadow Matching and GNSS Ranging aided by 3D Mapping," in *Proceedings of ION GNSS+ 2016*, Portland, September 2016.

[28] R. Kumar and M. G. Petovello, "A novel GNSS positioning technique for improved accuracy in urban canyon scenarios using 3D city model," in *Proceedings of the 27th International Technical Meeting of the Satellite Division of the Institute of Navigation (ION GNSS+ 2014), Tampa, FL, USA*, vol. 812, 2014, p. 21392148.

[29] T. Suzuki and N. Kubo, "Correcting GNSS multipath errors using a 3D surface model and particle filter," *Proc. ION GNSS+ 2013*, 2013.

[30] N. Kbayer and M. Sahmoudi, "Constructive Use of MP/NLOS bias of GNSS Pseudoranges: Performance Analysis by Type of Environment," in *Proceedings of the 2017 International Technical Meeting of The Institute of Navigation, ITM 2017*, January 2017.

[31] T. Chapuis, B. Bonhoure, F. Lacoste, C. Boulanger, D. Lapeyre, K. Urbanska, P. Noirat, and A. Marion, "SPRING simulator A powerful 3D computing engine toward urban canyons modelling," in *Satellite Navigation Technologies and European Workshop on GNSS Signals and Signal Processing,(NAVITEC), 2012 6th ESA Workshop on*. IEEE, 2012, pp. 1–8.

[32] M. Ait-Ighil, "Enhanced Physical Statistical Simulator of the Land Mobile Satellite Channel for Multipath Modelling Applied to Satellite Navigation Systems," 2013.

[33] M. Ait-Ighil, J. Lemorton, F. Pérez-Fontán, F. Lacoste, G. Artaud, C. Bourga, and M. Bousquet, "Simplifying the propagation environment representation for LMS channel modelling," *EURASIP Journal on Wireless Communications and Networking*, vol. 2012, no. 1, p. 110, 2012.

[34] T. Chapuis, B. Bonhoure, , S. Rougerie, F. Lacoste, T. Grelier, D. Lapeyre, and P. Noirat, "SPRING: A Powerful 3D GNSS Simulator for Constraint Environment," in *Proceedings of the 27th International Technical Meeting of The Satellite Division of the Institute of Navigation (ION GNSS+ 2014)*, September 2014, pp. 454 – 465.

[35] P. Misra and P. Enge, *Global Positioning System: Signals, Measurements, and Performance*, 2nd ed. Ganga-Jamuna Press, Lincoln MA, 2006.

[36] P. D. Groves, "Shadow Matching: A New GNSS Positioning Technique for Urban Canyons," *Journal of Navigation*, vol. 64, no. 3, 2011.

[37] ——, "Shadow matching: A new GNSS positioning technique for urban canyons," *Journal of Navigation*, vol. 64, no. 03, pp. 417–430, 2011.

[38] A. Irish, J. Isaacs, D. Iland, J. Hespanha, E. Belding, and U. Madhow, "Demo: ShadowMaps, the urban phone tracking system," in *Proceedings of the 20th annual international conference on Mobile computing and networking*. ACM, 2014, pp. 283–286.

[39] L. Wang, P. D. Groves, and M. K. Ziebart, "Urban positioning on a smartphone: Real-time shadow matching using GNSS and 3D city models." The Institute of Navigation, 2013.